

**Computing Quantities of Interest
for Random Domains with
Second Order Shape
Sensitivity Analysis**

M. Dambrine, H. Harbrecht, B. Puig

Institute of Mathematics
University of Basel
Rheinsprung 21
CH - 4051 Basel
Switzerland

Preprint No. 2014-13
September, 2014

www.math.unibas.ch

Computing quantities of interest for random domains with second order shape sensitivity analysis

M. Dambrine, H. Harbrecht, B. Puig

Abstract

We consider random perturbations of a given domain. The characteristic amplitude of these perturbations is assumed small. We are interested in quantities of interest depending on the random domain through a boundary value problem. We provide asymptotic expansions of the first moments of the distribution of this output function. When the random perturbation has a small rank spectral representation, we give a simple and efficient method to compute the coefficients of these expansions and provide numerical illustrations in order to compare our expansions with Monte Carlo simulations.

2000MSC : 60G35, 65N75, 65N99.

Keywords: random domains, second order shape sensitivity, low-rank approximations.

1 Introduction

Many practical problems in engineering lead to boundary value problem for an unknown function that is necessary to compute to obtain a real quantity of interest. In structural mechanics, the equations of elasticity are usually considered and solved to compute the leading mode of a structure or its compliance. Usually, the input parameters of the model like the geometry or the physical coefficients (typically the value of the Young modulus or Poisson ratio) are not known perfectly. It is therefore important to take these uncertainties into account.

In this work, we consider uncertainties on the geometric definition of the domain motivated by tolerances in the fabrication processes or in a damaged boundary during the life of a mechanical device. Manufactured devices are close to a nominal geometry but differ of course from its mathematical definition. Since we are motivated by tolerances, we can make the crucial assumption of the *smallness of the random perturbations*. Identifying domains with their boundary, domains close to the nominal domain D_0 can be seen as a normal perturbation of the nominal boundary ∂D . In that case, the random domain $D(\omega)$ can be defined thanks to a real valued random field X over ∂D according to

$$\partial D(\omega) = \{x + X(x, \omega)\mathbf{n}(x); \quad x \in \partial D_0\}.$$

In order to take the question of uncertain geometrical definition into account in numerical simulations, we have to incorporate the randomness of the computational domain to the underlying model equations. Thus, the quantities of engineering interest are also random. We address the following question: *given a complete probabilistic description of the random perturbation of the nominal boundary, compute as much information as possible to the distribution of the quantity of interest.*

The most common approach to study boundary value problems with stochastic inputs is the Monte-Carlo method. Often this approach is easy to implement and generates a sufficiently large number of samples. In our case, each sample is a realization of the random domain. On these samples, one

has to solve a boundary value problem and then to compute the quantity of interest. Therefore, the Monte-Carlo method is extremely costly. This work is a contribution to the *development of cheap and deterministic numerical methods to recover statistical informations on the distribution of the output quantity of interest*.

The smallness assumption formalized in the sequel allows us to use a sensitivity analysis with respect to geometrical perturbations of the boundary. We apply shape calculus to perform this sensitivity analysis of order two and compute asymptotic expansions of the moments of the output quantity distribution with respect to the smallness parameter ε of the random perturbations. In particular, we obtain in this work an expansion at order three for the expectation and an expansion of order four for the variance. It turns out that the leading coefficients of these asymptotic expansions do only depend on the autocovariance of the random field defining the random perturbations. We therefore use the associated integral operator to derive a low-rank approximation of the random field of the type

$$X(x, \omega) = \sum_{\mathbb{N}=1}^N \alpha_{\mathbb{N}}(\omega) f_{\mathbb{N}}(x).$$

For such a random field, we derive an analytic expression of the coefficients of the previous asymptotic expansions that are very cheap to compute: only $N + 1$ boundary values problems are to be solved on the nominal geometry D in the examples we present in this work. Note that when the derivative are evaluated thanks to an adjoint state, then $2N + 2$ problems are needed.

We mention that random shape functionals have also been considered in [7] by means of a first order perturbation analysis. A rather general framework of the first order perturbation analysis for functionals with random input parameters, particularly random domains, has been presented [1]. Nevertheless, the present paper is based on a second order perturbation analysis of the random shape functional under consideration. Thus, the shape Hessian will enter the asymptotic expansions which makes the computations much harder. However, the shape Hessian is meanwhile well understood and has been considered for example in [2, 3, 5, 8, 13, 15]. In comparison to [7], we derive here a more precise expansion of the random shape functional. This fact is also verified by our numerical experiments.

This work is organized as follows. In Section 2, we introduce our main theoretical tool: the shape calculus of order two. We define the shape derivative, present their structure theorem and their expressions in the case of two model objectives which we will focus on in this work: the first eigenvalue of the Dirichlet Laplace operator and the Dirichlet energy. Then, in Section 3, we detail our random model and explain how one can obtain in general asymptotic expansions of the moments of the quantity of interest distribution. In Section 4, we emphasize the role of the autocovariance of the field X to compute the previously derived asymptotic expansions and explain how to obtain a low-rank approximation of the field X itself. In Section 5, we make explicit the expansions of Section 3 and obtain expressions directly workable for computations. Finally, we validate our theoretical findings in Section 6 by comparing our results with Monte-Carlo simulations.

2 Second order shape calculus

2.1 Definitions and structure theorem

Shape calculus was founded by Hadamard a century ago but was really developed from the seventies on with the works of Murat and Simon as well as Sokolowski and Zolesio. It's objective is to provide a differential calculus for functions depending on the geometry of a domain D . It is achieved through

the action of a family of diffeomorphisms acting on a model domain. We refer readers interested in the precise definitions and useful properties to modern books on the subject such as [4, 8].

It is well-known since Hadamard's work that the shape gradient is a distribution supported on the moving boundary and acting on the normal component of the deformation field. The second order shape derivative also has a specific structure as stated by Pierre and Novruzi in [13]. We quote their result.

Theorem 2.1 (Structure theorem of first and second shape derivatives) *Let $k \geq 1$ be an integer and J a real valuated shape function defined \mathcal{O}_k the open bounded domains of \mathbb{R}^d with a \mathcal{C}^k boundary. Let us define the function \mathcal{J} on $\mathcal{C}^{k,\infty}(\mathbb{R}^d, \mathbb{R}^d)$ by*

$$\mathcal{J}(\theta) = J((I + \theta)(D)).$$

(i) *If $D \in \mathcal{O}_{k+1}$ and \mathcal{J} is differentiable at 0, then there exists a continuous linear form L on $\mathcal{C}^k(\partial D)$ such that:*

$$D\mathcal{J}(0)\xi = L(\xi \cdot \mathbf{n}) \text{ for all } \xi \in \mathcal{C}^{k,\infty}(\mathbb{R}^d, \mathbb{R}^d).$$

(ii) *If $D \in \mathcal{O}_{k+2}$ and \mathcal{J} is twice differentiable at 0, then there exists a continuous symmetric bilinear form B on $\mathcal{C}^k(\partial D) \times \mathcal{C}^k(\partial D)$ such that for all $(\xi, \zeta) \in \mathcal{C}^{k,\infty}(\mathbb{R}^d, \mathbb{R}^d)^2$*

$$D^2\mathcal{J}(0)(\xi, \zeta) = B(\xi \cdot \mathbf{n}, \zeta \cdot \mathbf{n}) + L((D_\tau \mathbf{n} \zeta_\tau) \cdot \xi_\tau - \nabla_\tau (\zeta \cdot \mathbf{n}) \cdot \xi_\tau - \nabla_\tau (\xi \cdot \mathbf{n}) \cdot \zeta_\tau),$$

where ∇_τ is the tangential gradient and ξ_τ and ζ_τ stands for the tangential components of ξ and ζ .

The so-called shape derivative are then the shape gradient, usually noted $DJ(D) := D\mathcal{J}(0)$, and the shape Hessian, usually noted $D^2J(D) := D^2\mathcal{J}(0)$. With respect to this work, it is important to notice that the shape Hessian is reduced to B for normal deformations fields.

Following the structure theorem, let us consider a \mathcal{C}^4 domain D_0 and consider a \mathcal{C}^3 neighborhood \mathcal{O} of D and a twice differentiable shape function J . If the size of the neighborhood is small enough, the local inversion theorem shows that the boundary ∂D of any domain D in \mathcal{O} can be represented as a graph over ∂D_0 of the form: there is a real valuted function φ defined on ∂D_0 such that

$$\partial D = \{x + \varphi(x)\mathbf{n}(x); \ x \in \partial D_0\}.$$

In particular, one can restrict themself to normal perturbations of amplitude φ , and for a given function φ defined on ∂D_0 , define a domain D_φ as the interior of the set $\{x + \varphi(x)\mathbf{n}(x); \ x \in \partial D_0\}$. Then one obtains the Taylor formula

$$J(D_\varphi) = J(D_0) + L[J](D_0)\varphi + \frac{1}{2}B[J](D_0)(\varphi, \varphi) + R_2(\varphi), \quad (1)$$

where the reminder R_2 is uniformly in φ negligible with respect to $\|\varphi\|^2$.

2.2 Examples of shapes derivatives.

We need to precise some geometrical definitions. The mean curvature (understood as the sum of the principal curvatures of ∂D) is denoted by H . For a domain $D \subset \mathbb{R}^d$, we consider its Dirichlet energy $E(D)$ defined as

$$E(D) = -\frac{1}{2} \int_{\partial D} |\nabla u_D|^2,$$

where u_D is the solution of $-\Delta u = 1$ in $H_0^1(D)$ and λ_1 the first eigenvalue of the Dirichlet Laplace operator. The shape derivatives of these functionals are well-known (see [8, Section 5.9.6]).

Lemma 2.2 (Expressions of shape derivatives) *If D is \mathcal{C}^2 , one has*

$$L[E](D).\varphi = -\frac{1}{2} \int_{\partial D} (\partial_n u)^2 \varphi; \quad (2a)$$

$$B[E](D).(\varphi, \varphi) = \langle -\partial_n u \varphi, \Lambda(-\partial_n u \varphi) \rangle_{\mathbb{H}^{1/2} \times \mathbb{H}^{-1/2}} + \int_{\partial D} \left[\partial_n u + \frac{1}{2} H(\partial_n u)^2 \right] \varphi^2; \quad (2b)$$

$$L[\lambda_1](D).\varphi = - \int_{\partial D} (\partial_n v)^2 \varphi; \quad (2c)$$

$$B[\lambda_1](D).(\varphi, \varphi) = \int_{\partial D} 2w(\varphi) \partial_n w(\varphi) + H(\partial_n v)^2 \varphi^2; \quad (2d)$$

where $\Lambda : \mathbb{H}^{1/2}(\partial D) \rightarrow \mathbb{H}^{-1/2}(\partial D)$ is the Dirichlet-to-Neumann map for the domain D defined as $\Lambda(\varphi) = -\partial_n V(\varphi)$ with $V(\varphi)$ being the solution of

$$-\Delta V(\varphi) = 0 \text{ in } D, \quad V(\varphi) = -\varphi \text{ on } \partial D, \quad (3)$$

and v is the associated normalized eigenfunction solution in $\mathbb{H}_0^1(D)$ of $-\Delta v = \lambda_1 v$ with $v > 0$ in D and $w(\varphi)$ is the solution of

$$\begin{cases} -\Delta w(\varphi) = \lambda_1 w(\varphi) - v \int_{\partial D} (\partial_n v)^2 \varphi \text{ in } D, \\ w(\varphi) = -\varphi \partial_n v \text{ on } \partial D, \\ \int_D v w(\varphi) = 0. \end{cases} \quad (4)$$

As consequence of these examples and being the general case to the best of our knowledge, there is a function ℓ defined on ∂D so that the shape gradient can be written as

$$L(D).\varphi = \int_{\partial D} \ell \varphi. \quad (5)$$

This property to be an integral operator with a nice kernel is not true in general for the second order derivative.

3 Asymptotic expansions of the moments

3.1 The stochastic model: random graphs over a fixed domain's boundary.

For modeling the stochastic perturbations $D(\cdot)$ of D_0 , we introduce a probability space $(\Omega, \mathcal{F}, \mathbb{P})$ and consider stochastic functions $X : \partial D_0 \times \Omega \rightarrow \mathbb{R}$ that define $D(\omega)$ as the interior of the graph $x + X(x, \omega) \mathbf{n}_{\partial D_0}(x)$. In order to keep a pertinent geometrical description of sets, this of course requires that the domains $D(\omega)$ remain close to D_0 at least in the \mathbb{L}^∞ sense. In fact, to use the expansion (1), we need closeness in the \mathcal{C}^2 sense. Introducing a small parameter $\varepsilon > 0$ and plugging perturbations of the form $x + \varepsilon X(x, \omega) \mathbf{n}_{\partial D_0}(x)$ into (1), we obtain

$$J(D(\omega)) = J(D_0) + \varepsilon L(X(\omega)) + \frac{\varepsilon^2}{2} B(X(\omega), X(\omega)) + R_2(\varepsilon X(\omega)). \quad (6)$$

We make the assumption that X is uniformly (in ω) bounded in the norm in the spatial variable where shape differentiability holds at the second order (typically here the \mathcal{C}^2 norm), i.e., X is a member of the Bochner space $\mathbb{L}^\infty(\Omega, \mathcal{C}^2(\partial D_0))$. Then, there exists $C > 0$ such that $|R_2(\varepsilon X(\omega))| \leq C \varepsilon^3$.

3.2 General preliminary results.

In view of (6), we derive the asymptotic expansions of the expectation and variance of $J(D(\omega))$ as our first result.

Proposition 3.1 *The expectation and variance of $J(D(\omega))$ admit the asymptotic expansions*

$$\mathbb{E}(J(D)) = J(D_0) + \varepsilon \mathbb{E}(L(X)) + \frac{\varepsilon^2}{2} \mathbb{E}(B(X, X)) + \mathcal{O}(\varepsilon^3) \quad (7)$$

and

$$\begin{aligned} \text{var}(J(D)) &= \varepsilon^2 \mathbb{E} \left([L(X) - \mathbb{E}(L(X))]^2 \right) \\ &\quad + \varepsilon^3 \mathbb{E} \left([L(X) - \mathbb{E}(L(X))] [B(X, X) - \mathbb{E}(B(X, X))] \right) + \mathcal{O}(\varepsilon^4). \end{aligned} \quad (8)$$

Proof of Proposition 3.1. It suffices to integrate over the space of probability the pointwise Taylor expansion (6) thanks to the uniform estimate of the reminder. One thus immediately obtains for the expectation

$$\begin{aligned} \mathbb{E}(J(D)) &= J(D_0) + \varepsilon \mathbb{E}(L(X)) + \frac{\varepsilon^2}{2} \mathbb{E}(B(X, X)) + \mathbb{E}(R_2(\varepsilon X)) \\ &= J(D_0) + \varepsilon \mathbb{E}(L(X)) + \frac{\varepsilon^2}{2} \mathbb{E}(B(X, X)) + \mathcal{O}(\varepsilon^3). \end{aligned}$$

Likewise, for the variance, one has

$$\begin{aligned} \text{var}(J(D)) &= \mathbb{E} \left([J(D) - \mathbb{E}(J(D))]^2 \right) \\ &= \mathbb{E} \left(\left[\varepsilon(L(X) - \mathbb{E}(L(X))) + \frac{\varepsilon^2}{2}(B(X, X) - \mathbb{E}(B(X, X))) + \mathcal{O}(\varepsilon^3) \right]^2 \right) \\ &= \varepsilon^2 \mathbb{E} \left([L(X) - \mathbb{E}(L(X))]^2 \right) + \varepsilon^3 \mathbb{E} \left([L(X) - \mathbb{E}(L(X))] [B(X, X) - \mathbb{E}(B(X, X))] \right) + \mathcal{O}(\varepsilon^4). \end{aligned}$$

■

Remark 3.2 Let us notice that it follows $\mathbb{E}(L(X)) = L(\mathbb{E}(X)) = 0$ if X is centered, i.e., if $\mathbb{E}(X) = 0$.

In the same spirit as above, we can also compute asymptotic expansions of higher moments. For example, the centered, normalized moments (as Skewness and Kurtosis) could be obtained in the following way.

Proposition 3.3 *For all $k \geq 2$, the centered normalized moment of $J(D(\omega))$ admits the asymptotic expansion*

$$\mathbb{M}_k(J(D)) := \mathbb{E} \left(\frac{[J(D) - \mathbb{E}(J(D))]^k}{\sqrt{\text{var}(J(D))}^k} \right) = a_k + b_k \varepsilon + \mathcal{O}(\varepsilon^2), \quad (9)$$

where the deterministic coefficients a_k and b_k are

$$a_k = \gamma_k \mathbb{E} \left([L(X) - \mathbb{E}(L(X))]^k \right) \mathbb{E} \left([L(X) - \mathbb{E}(L(X))]^2 \right), \quad (10)$$

$$\begin{aligned} b_k &= \gamma_k \left\{ \mathbb{E} \left([L(X) - \mathbb{E}(L(X))]^{k-1} [B(X, X) - \mathbb{E}(B(X, X))] \right) \mathbb{E} \left([L(X) - \mathbb{E}(L(X))]^2 \right) \right. \\ &\quad \left. - \mathbb{E} \left([L(X) - \mathbb{E}(L(X))] [B(X, X) - \mathbb{E}(B(X, X))] \right) \mathbb{E} \left([L(X) - \mathbb{E}(L(X))]^k \right) \right\}, \end{aligned} \quad (11)$$

and the normalization constant γ_k is

$$\gamma_k = \mathbb{E} \left([L(X) - \mathbb{E}(L(X))]^2 \right)^{-1-k/2}. \quad (12)$$

Proof of Proposition 3.3. We have

$$\frac{1}{\sqrt{x+h}^k} = \frac{1}{\sqrt{x}^k} - \frac{hk}{2\sqrt{x}^{k+2}} + \mathcal{O}(h^2).$$

Inserting the expansion of the variance (8), we find

$$\begin{aligned} \frac{1}{\sqrt{\text{var}(J(D))}^k} &= \frac{1}{\varepsilon^k} \left\{ \mathbb{E} \left([L(X) - \mathbb{E}(L(X))]^2 \right)^{-k/2} \right. \\ &\quad - \frac{\varepsilon k}{2} \mathbb{E} \left([L(X) - \mathbb{E}(L(X))]^2 \right)^{-1-k/2} \mathbb{E} \left([L(X) - \mathbb{E}(L(X))] [B(X, X) - \mathbb{E}(B(X, X))] \right) \\ &\quad \left. + \mathcal{O}(\varepsilon^2) \right\}. \end{aligned}$$

On the other hand, using the expansion of the expectation (7), we have

$$\begin{aligned} \mathbb{E} \left([J(D) - \mathbb{E}(J(D))]^k \right) &= \varepsilon^k \left\{ \mathbb{E} \left([L(X) - \mathbb{E}(L(X))]^k \right) \right. \\ &\quad \left. + \frac{\varepsilon k}{2} \mathbb{E} \left([L(X) - \mathbb{E}(L(X))]^{k-1} [B(X, X) - \mathbb{E}(B(X, X))] \right) + \mathcal{O}(\varepsilon^2) \right\}. \end{aligned}$$

Then, a tedious but elementary calculus (the product of two asymptotic expansions) leads to the desired result. ■

4 Computation of the expansion coefficients. The general case.

4.1 Direct computation

For sake of simplicity, we shall assume that the boundary perturbation field X is centered which induces $\mathbb{E}(L(X)) = 0$. We then can compute as in [7]

$$\begin{aligned} \mathbb{E} \left([L(X) - \mathbb{E}(L(X))]^2 \right) &= \mathbb{E} \left(L(X)^2 \right) = \mathbb{E} \left[\left(\int_{\partial D_0} \ell(x) X(x, \omega) d\sigma(x) \right)^2 \right] \\ &= \mathbb{E} \left[\int_{\partial D_0} \int_{\partial D_0} X(x, \omega) X(y, \omega) \ell(x) \ell(y) d\sigma(x) d\sigma(y) \right] \\ &= \int_{\partial D_0} \int_{\partial D_0} \mathbb{E} [X(x, \cdot) X(y, \cdot)] \ell(x) \ell(y) d\sigma(x) d\sigma(y). \end{aligned}$$

The crucial operator to be studied here is the (two-point) autocovariance function of X defined as

$$\text{Cov}_X(x, y) = \mathbb{E}(X(x, \cdot) X(y, \cdot)).$$

In fact, the knowledge of the law of X is not needed for the computation we have in mind, we only need the autocovariance function. Notice that various laws for X can provide the same function Cov_X .

We can proceed in two different ways to compute the expectation of the shape Hessian. The first approach has already been pointed out in e.g. [12]. We shall explain the proceeding in case of the Dirichlet energy. In that case, according to (2b), we have

$$\mathbb{E}(B(X, X)) = \mathbb{E} \left(\int_{\partial D_0} \left[\partial_n u + \frac{1}{2} H(\partial_n u)^2 \right] X^2 \right) + \mathbb{E} \left(\langle -\partial_n u X, \Lambda(-\partial_n u X) \rangle_{H^{1/2} \times H^{-1/2}} \right).$$

For the first term, one has easily by Fubini's theorem that

$$\mathbb{E} \left(\int_{\partial D} \left[\partial_n u + \frac{1}{2} H(\partial_n u)^2 \right] X^2 \right) = \int_{\partial D_0} \mathbb{E}(X^2) \left[\partial_n u + \frac{1}{2} H(\partial_n u)^2 \right] = \int_{\partial D_0} \mathbb{V}(X) \left[\partial_n u + \frac{1}{2} H(\partial_n u)^2 \right]$$

since X is centered. To compute the second term, we shall define the following tensor product type boundary value problem:

$$\begin{aligned} (id \otimes (-\Delta))V &= 0 && \text{in } \partial D_0 \times D_0, \\ V &= \text{Cov}_X(id \otimes (-\partial_n u)) && \text{on } \partial D_0 \times \partial D_0. \end{aligned} \tag{13}$$

Note that the differential operator which underlies this boundary value problem is $id \otimes \Lambda$. Due to its linearity and Fubini's theorem, we get thus for the second term

$$\begin{aligned} \mathbb{E} \left(\langle -\partial_n u X, \Lambda(-\partial_n u X) \rangle_{H^{1/2} \times H^{-1/2}} \right) &= \int_{\partial D_0} \mathbb{E} \left(-\partial_n u(x) X(x, \cdot) (\Lambda(-\partial_n u X))(y, \cdot) \Big|_{x=y} \right) d\sigma(x) \\ &= \int_{\partial D_0} -\partial_n u(x) V(x, y) \Big|_{x=y} \sigma(x). \end{aligned}$$

Boundary value problems like that in (13) can be solved in essentially linear complexity if a sparse tensor product discretization is employed as proposed in e.g. [9, 11, 12]. However, the implementation of this approach would be highly intrusive.

4.2 Toward a low-rank approximation

The second way, which is much simpler to implement, consists in computing an expansion of the autocovariance function of X of the form

$$\text{Cov}_X = \sum_k \kappa_k \otimes \kappa_k. \tag{14}$$

For example, such a representation can be achieved by a spectral decomposition as an application of Mercer's theorem that ensures the representation of Cov_X in the form

$$\text{Cov}_X(x, y) = \sum_k \lambda_k e_k(x) e_k(y). \tag{15}$$

Another way to obtain such a decomposition is an (possibly infinite) Cholesky decomposition of autocovariance function. With the expansion (14) at hand, we will obtain in Section 5 the following expansion of the expectation of the shape Hessian:

$$\mathbb{E}(B[J](D_0)[X, X]) = \sum_k B[J](D_0)[\kappa_k, \kappa_k].$$

We therefore need only to be able to evaluate the shape Hessian in certain directions $\{\kappa_i\}$.

4.3 Numerical realization

In practice, the expansion (14) will be infinite and has to be appropriately truncated for numerical computations. Consider a suitable ansatz space $V_n = \text{span}\{\varphi_i : i = 1, 2, \dots, n\} \subset \mathcal{C}^2(\partial D_0)$. Then, we shall discretize the two-point correlation $\text{Cov}_X \in L^2(\partial D_0 \times \partial D_0)$ in the tensor product space $V_n \otimes V_n$ which yields the matrix

$$\mathbf{C} = \left[\int_{\partial D_0} \int_{\partial D_0} \text{Cov}_X(x, y) \varphi_i(x) \varphi_j(y) d\sigma(x) d\sigma(y) \right]_{i,j} \in \mathbb{R}^{n \times n}. \quad (16)$$

The discrete version of the expansion (14) is now efficiently be derived by an appropriate low-rank decomposition of this matrix, i.e.,

$$\mathbf{C} \approx \mathbf{C}_m = \sum_{k=1}^m \boldsymbol{\ell}_k \boldsymbol{\ell}_k^T, \quad (17)$$

where the truncation error $\|\mathbf{C} - \mathbf{C}_m\|$ should be rigorously controllable. Namely, with the low-rank decomposition (17) and the mass matrix

$$\mathbf{G} = \left[\int_{\partial D_0} \int_{\partial D_0} \varphi_i(x) \varphi_j(y) d\sigma(x) d\sigma(y) \right]_{i,j} \in \mathbb{R}^{n \times n}$$

with respect to the ansatz space V_n at hand, we have

$$\text{Cov}_X(x, y) \approx \sum_{k=1}^m \left(\sum_{i=1}^n \tilde{\ell}_{k,i} \varphi_i(x) \right) \left(\sum_{j=1}^n \tilde{\ell}_{k,j} \varphi_j(y) \right) \quad \text{with} \quad \tilde{\boldsymbol{\ell}}_k = [\tilde{\ell}_{k,i}]_i = \mathbf{G}^{-1} \boldsymbol{\ell}_k.$$

The best low-rank approximation in $L^2(\partial D_0 \times \partial D_0)$ is given by truncating the spectral decomposition (15). The computation requires the knowledge of the eigenpairs (φ_i, λ_i) of the integral operator

$$(\mathcal{C}u)(x) := \int_{\partial D_0} \text{Cov}_X(x, y) u(y) d\sigma(y), \quad x \in \partial D_0 \quad (18)$$

which is a very demanding task. In particular, the decay of the eigenvalues $\{\lambda_k\}$ and thus the rank m depend heavily on the smoothness of the autocovariance function Cov_X . Related decay rates have been proven in [16].

We propose to use the pivoted Cholesky decomposition to compute a low-rank approximation of Cov_X as proposed in [10]. It is a purely algebraic approach which is quite simple to implement, see Algorithm 1. It produces a low-rank approximation to \mathbf{C} for any given precision $\varepsilon > 0$ where the approximation error is rigorously controlled in the trace norm. A rank- m approximation is computed in $\mathcal{O}(m^2 n)$ operations. Exponential convergence rates in m are proven under the assumption that the eigenvalues of \mathbf{C} exhibit a sufficiently fast exponential decay, see [10]. Nevertheless, numerical experiments show that, in general, the pivoted Cholesky decomposition converges optimally in the sense that the rank m is uniformly bounded by the number of terms required for the spectral decomposition of Cov_X to get the error ε .

5 Computing the coefficients for a low-rank approximation of X

As a result of the pivoted Cholesky decomposition, we obtain a low-rank approximation on the random field X . Given N smooth real valued functions f_N defined on ∂D_0 , eventually with compact support on ∂D_0 if needed, we consider the domains defined by their boundary

$$\partial D_\varepsilon(\omega) = \left\{ x + \varepsilon X(x, \omega) \mathbf{n}(x); X \in \partial D_0 \right\}, \quad (19)$$

Algorithm 1: Pivoted Cholesky decomposition

Data: matrix $\mathbf{C} = [c_{i,j}]_{i,j} \in \mathbb{R}^{n \times n}$ and error tolerance $\varepsilon > 0$

Result: low-rank approximation $\mathbf{C}_m = \sum_{i=1}^m \ell_i \ell_i^T$ such that $\text{trace}(\mathbf{C} - \mathbf{C}_m) \leq \varepsilon$

begin

 set $m := 1$;

 set $\mathbf{d} := \text{diag}(\mathbf{C})$ and $\text{error} := \|\mathbf{d}\|_1$;

 initialize $\boldsymbol{\pi} := (1, 2, \dots, n)$;

while $\text{error} > \varepsilon$ **do**

 set $i := \arg \max\{d_{\pi_j} : j = m, m+1, \dots, n\}$;

 swap π_m and π_i ;

 set $\ell_{m,\pi_m} := \sqrt{d_{\pi_m}}$;

for $m+1 \leq i \leq n$ **do**

 compute $\ell_{m,\pi_i} := \left(c_{\pi_m,\pi_i} - \sum_{j=1}^{m-1} \ell_{j,\pi_m} \ell_{j,\pi_i} \right) / \ell_{m,\pi_m}$;

 update $d_{\pi_i} := d_{\pi_i} - \ell_{m,\pi_m} \ell_{m,\pi_i}$;

 compute $\text{error} := \sum_{i=m+1}^n d_{\pi_i}$;

 increase $m := m+1$;

end

with

$$X(x, \omega) = \sum_{\aleph=1}^N \alpha_{\aleph}(\omega) f_{\aleph}(x) \quad (20)$$

where the α_{\aleph} are independent and identically distributed following the same centered distribution \mathcal{L} of a random variable α . Note that such a model can also be provided by the Karhunen-Loève expansion. Nevertheless, for the the third order term of the expansion of the variance (see (24)) we make the assumption that the α_{\aleph} are independent and not only decorrelated.

In that case, the expansion coefficients can be very easily computed: the computational cost reduces to $N+1$ resolutions of boundary values problems defined on the same domain so that a single mesh can be used. This amount doubles to $2N+2$ resolutions in case of general shape functionals where also an adjoint state has to be computed.

Proposition 5.1 *When the random graph has the form (19), one has*

$$\mathbb{E}(J(D)) = J(D_0) + \frac{\varepsilon^2}{2} \mathbb{E}(\alpha^2) \sum_{\aleph=1}^N B(f_{\aleph}, f_{\aleph}) + \mathcal{O}(\varepsilon^3) \quad (21)$$

and

$$\text{var}(J(D)) = \varepsilon^2 \mathbb{E}(\alpha^2) \sum_{\aleph=1}^N (L(f_{\aleph}))^2 + \varepsilon^3 \mathbb{E}(\alpha^3) \sum_{\aleph=1}^N L(f_{\aleph}) B(f_{\aleph}, f_{\aleph}) + \mathcal{O}(\varepsilon^4). \quad (22)$$

Moreover, if the random variable α is symmetric, it even holds

$$\text{var}(J(D)) = \varepsilon^2 \mathbb{E}(\alpha^2) \sum_{\aleph=1}^N (L(f_{\aleph}))^2 + \mathcal{O}(\varepsilon^4). \quad (23)$$

Proof of Proposition 5.1. Note that we give the proof in full details for the generic case of the Dirichlet energy to simplify notations. This case presents all the difficulties, one has to face.

1. *Expansion of the expectation.* By linearity, it comes directly

$$\mathbb{E}(L(X)) = L(\mathbb{E}(X)) = 0.$$

Concerning the order two coefficient, a difficulty appears since, in general, the shape Hessian B acting on normal components of deformations can be split in two parts: first a integral term involving the square of the normal deformation or of its derivatives and second a non local one involving a pseudodifferential operator.

Let us explain how to compute it on the significant example of Dirichlet energy. In that case, according to (2b),

$$\mathbb{E}(B(X, X)) = \mathbb{E} \left(\int_{\partial D_0} \left[\partial_n u + \frac{1}{2} H(\partial_n u)^2 \right] X^2 \right) + \mathbb{E} \left(\langle -\partial_n u X, \Lambda(-\partial_n u X) \rangle_{H^{1/2} \times H^{-1/2}} \right).$$

We recall that Λ denotes the Dirichlet-to-Neumann map defined via (3). On the one hand, one has easily by Fubini's theorem and the choice of α_{\aleph} are independent and centered:

$$\begin{aligned} \mathbb{E} \left(\int_{\partial D_0} \left[\partial_n u + \frac{1}{2} H(\partial_n u)^2 \right] X^2 \right) &= \int_{\partial D_0} \left[\partial_n u + \frac{1}{2} H(\partial_n u)^2 \right] \mathbb{E}(X^2) \\ &= \mathbb{E}(\alpha^2) \int_{\partial D_0} \left[\partial_n u + \frac{1}{2} H(\partial_n u)^2 \right] \sum_{\aleph=1}^N f_{\aleph}^2. \end{aligned}$$

On the other hand, due to the linearity of the Dirichlet-to-Neumann map which acts only on the spatial variable, we observe

$$\Lambda \left(\partial_n u \sum_{\aleph=1}^N \alpha_{\aleph}(\omega) f_{\aleph} \right) = \sum_{\aleph=1}^N \alpha_{\aleph}(\omega) \Lambda(\partial_n u f_{\aleph}).$$

Hence, it follows likewise by Fubini's theorem

$$\begin{aligned} \mathbb{E} \left(\langle -\partial_n u X, \Lambda(-\partial_n u X) \rangle_{H^{1/2} \times H^{-1/2}} \right) &= \mathbb{E} \left(\sum_{\aleph_1=1}^N \sum_{\aleph_2=1}^N \alpha_{\aleph_1} \alpha_{\aleph_2} \langle \partial_n u f_{\aleph_1}, \Lambda(\partial_n u f_{\aleph_2}) \rangle_{H^{1/2} \times H^{-1/2}} \right) \\ &= \mathbb{E}(\alpha^2) \sum_{\aleph=1}^N \langle -\partial_n u f_{\aleph}, \Lambda(-\partial_n u f_{\aleph}) \rangle_{H^{1/2} \times H^{-1/2}}. \end{aligned}$$

2. *Expansion of the variance.* We first have

$$\begin{aligned} \mathbb{E} \left([L(X) - \mathbb{E}(L(X))]^2 \right) &= \int_{\partial D_0} \int_{\partial D_0} \mathbb{E}(X(x, \cdot) X(y, \cdot)) \ell(x) \ell(y) d\sigma(x) d\sigma(y) \\ &= \mathbb{E}(\alpha^2) \sum_{\aleph=1}^N \int_{\partial D_0} \int_{\partial D_0} \ell(x) \ell(y) f_{\aleph}(x) f_{\aleph}(y) d\sigma(x) d\sigma(y) = \mathbb{E}(\alpha^2) \sum_{\aleph=1}^N (L(f_{\aleph}))^2. \end{aligned}$$

where we used the notation introduced in (5) and Fubini's theorem. Second, we have to compute

$$A = \mathbb{E}([L(X) - \mathbb{E}(L(X))] [B(X, X) - \mathbb{E}(B(X, X))]) = \mathbb{E}(L(X)B(X, X))$$

since $\mathbb{E}(L(X)) = 0$. We split the shape Hessian as previously into an integral over the boundary and the pseudo-differential term so that $A = A_1 + A_2$. We explicit the generic case of torsion:

$$A_1 = \mathbb{E} \left(\left[\int_{\partial D_0} \ell(x) \sum_{\aleph=1}^N \alpha_{\aleph} f_{\aleph}(x) d\sigma(x) \right] \left[\int_{\partial D_0} \left[\partial_n u(y) + \frac{1}{2} H(y) (\partial_n u(y))^2 \right] \left[\sum_{\aleph=1}^N \alpha_{\aleph} f_{\aleph}(y) \right]^2 d\sigma(y) \right] \right),$$

$$A_2 = \mathbb{E} \left(\left[\int_{\partial D_0} \ell(x) \sum_{\aleph=1}^N \alpha_{\aleph} f_{\aleph}(x) d\sigma(x) \right] \left[\sum_{\aleph_1=1}^N \sum_{\aleph_2=1}^N \alpha_{\aleph_1} \alpha_{\aleph_2} \langle \partial_n u f_{\aleph_1}, \Lambda(\partial_n u f_{\aleph_2}) \rangle_{\mathbb{H}^{1/2} \times \mathbb{H}^{-1/2}} \right] \right).$$

Applying Fubini's theorem, we obtain after expansion:

$$A_1 = \int_{\partial D_0} \int_{\partial D_0} \ell(x) \left[\partial_n u(y) + \frac{1}{2} H(y) (\partial_n u(y))^2 \right]$$

$$\times \sum_{\aleph_1=1}^N \sum_{\aleph_2=1}^N \sum_{\aleph_3=1}^N \mathbb{E}(\alpha_{\aleph_1} \alpha_{\aleph_2} \alpha_{\aleph_3}) f_{\aleph_1}(x) f_{\aleph_2}(y) f_{\aleph_3}(y) d\sigma(x) d\sigma(y),$$

$$A_2 = \int_{\partial D_0} \ell(x) \sum_{\aleph_1=1}^N \sum_{\aleph_2=1}^N \sum_{\aleph_3=1}^N \mathbb{E}(\alpha_{\aleph_1} \alpha_{\aleph_2} \alpha_{\aleph_3}) f_{\aleph_1}(x) \langle \partial_n u f_{\aleph_2}, \Lambda(\partial_n u f_{\aleph_3}) \rangle_{\mathbb{H}^{1/2} \times \mathbb{H}^{-1/2}} d\sigma(x).$$

Since the α_{\aleph} are independant, one has

$$\mathbb{E}(\alpha_{\aleph_1} \alpha_{\aleph_2} \alpha_{\aleph_3}) = 0 \text{ except if } \aleph_1 = \aleph_2 = \aleph_3. \quad (24)$$

We then arrive at

$$A_1 = \mathbb{E}(\alpha^3) \sum_{\aleph=1}^N L(f_{\aleph}) \int_{\partial D_0} \left[\partial_n u(y) + \frac{1}{2} H(y) (\partial_n u(y))^2 \right]^2 f_{\aleph}(y)^2 d\sigma(y);$$

$$A_2 = \mathbb{E}(\alpha^3) \sum_{\aleph=1}^N L(f_{\aleph}) \langle \partial_n u f_{\aleph}, \Lambda(\partial_n u f_{\aleph}) \rangle_{\mathbb{H}^{1/2} \times \mathbb{H}^{-1/2}}.$$

Gathering A_1 and A_2 , we obtain the claimed result. If the random variable α is symmetric, then $\mathbb{E}(\alpha^3) = 0$ and both terms A_1 and A_2 vanish. \blacksquare

Finally, using the Bienaymé-Chebychev inequality, we obtain intervals in which the Dirichlet energy takes its values with a fixed probability. For example, fixing a desired probability p , we get the bounds

$$\mathbb{P} \left(|J(D) - \mathbb{E}(J(D))| \leq \sqrt{\frac{\text{var}(J(D))}{1-p}} \right) \geq p.$$

Thanks to the asymptotic expansions (21)–(22), we obtain then

$$\mathbb{P} (J_{\varepsilon,p}^-(D) \leq J(D) \leq J_{\varepsilon,p}^+(D)) \geq p \quad (25)$$

where we have set

$$J_{\varepsilon,\alpha}^{\pm}(D) = J(D_0) \pm \frac{\varepsilon}{\sqrt{1-p}} \sqrt{\mathbb{E}(\alpha^2) \sum_{\aleph=1}^N (L(f_{\aleph}))^2}$$

$$+ \frac{\varepsilon^2}{2} \left(\mathbb{E}(\alpha^2) \sum_{\aleph=1}^N B(f_{\aleph}, f_{\aleph}) \pm \frac{\mathbb{E}(\alpha^3)}{\sqrt{1-p}} \sum_{\aleph=1}^N L(f_{\aleph}) B(f_{\aleph}, f_{\aleph}) \right) + \mathcal{O}(\varepsilon^3).$$

6 Numerical illustrations

We now present numerical validations of the proposed asymptotic expansions. We will consider two dimensional cases for the Dirichlet energy and the first eigenvalue of the Dirichlet-Laplace operator. Numerical resolution of the boundary values problems is made either with the finite elements either with boundary integral method. We will consider both uniform and Beta distribution. During the Monte-Carlo simulations, the random generator has been restarted after at most 10 000 samples.

6.1 The Dirichlet energy around disk in dimension two

6.1.1 The random domains

We consider the unit disk in the plane and random perturbations of the type

$$D_\varepsilon(\omega) = \left\{ (r, \theta) : 0 \leq r < 1 + \varepsilon f(\theta, \omega) \text{ and } f(\theta) = \sum_{\aleph=1}^N \alpha_\aleph(\omega) f_\aleph(x) \right\} \quad (26)$$

where the α_\aleph are i.i.d. In the following computations, we have taken $N = 11$ and the f_\aleph are the first normalized fonctions in the Fourier basis that is

$$f_1 = 1, f_2(\theta) = \cos(\theta), f_3(\theta) = \sin(\theta), f_4(\theta) = \cos(2\theta)/4, f_5(\theta) = \sin(2\theta)/4, \dots, f_{11}(\theta) = \sin(5\theta)/25.$$

Let us present some realisations of such domains with various values of ε and various distributions. In Figure 1, we present some realisations of such random domains for α following the uniform distribution on $[-1/2, 1/2]$: note that the range of α is $[-1/2, 1/2]$.

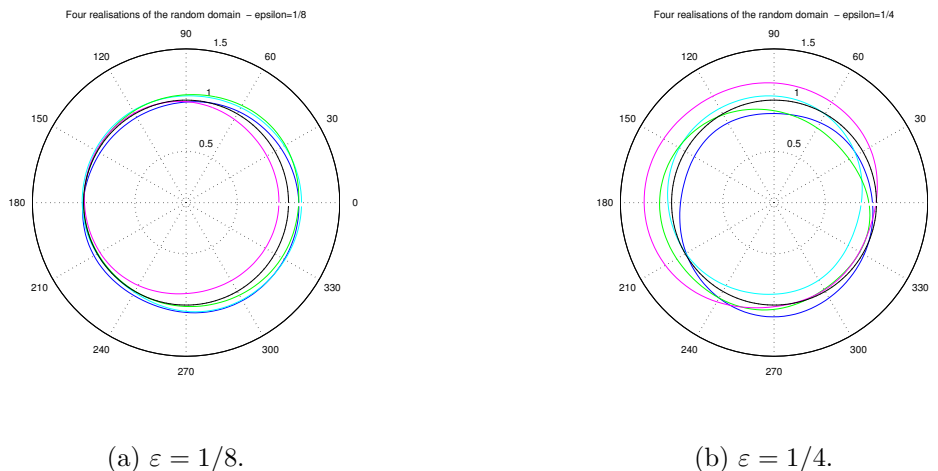


Figure 1: Some realisations of domains according to (26) with the uniform distribution.

In Figure 2, α follows the centered and normalized Beta distribution of parameter $(2, 5)$ in order to use a non symmetric distribution. Note that the range of this distribution is larger (it can take values greater than 4), so for the same value of the parameter ε the perturbations can be wider for the beta distribution than for the uniform distribution. Therefore, we will consider a smaller range of value of epsilon.

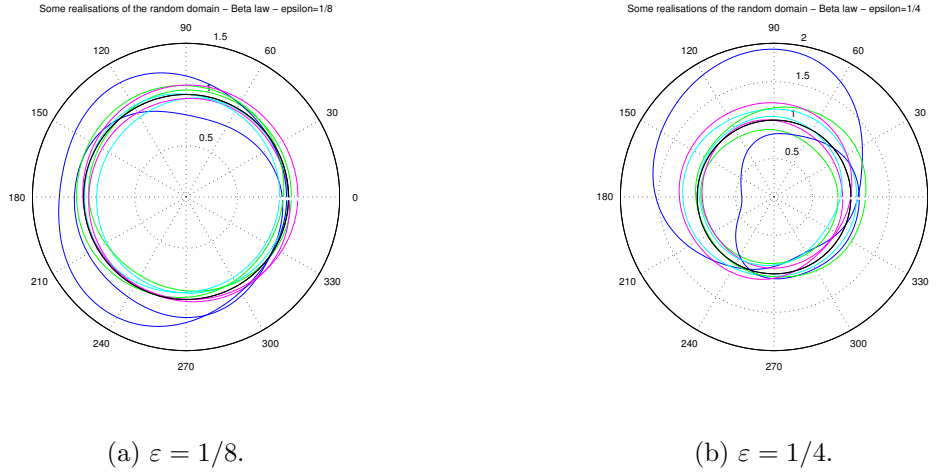


Figure 2: Some realisations of domains according to (26) with the beta distribution.

6.1.2 Monte-Carlo simulations

To check our expansion, we proceed to simulation with the Monte-Carlo method. For each value of ε in abscisse on the graphs, we proceed to 4000 simulations using $P1$ finite elements over around 2000 triangles each made with the FREEFEM++ code. The convergence is illustrated in Figure 3. It seems that a visually correct asymptotic regime is reached for some thousand of simulations.

6.1.3 Comparison with the asymptotic expansions

Finally, we compare with the asymptotic expansions obtained in Proposition 5.1. Let us emphasize that the coefficients appearing in (5.1) are computed numerically. The first step is to compute the state equation in the reference domain, then the shape gradient is obtained via the computation of an integral over the boundary. Finally, the computation of each term $B(f_N, f_N)$ requires the solution of a boundary value problem of the same type than the one solved for the state equation. Therefore, the computation of these coefficients is cheap since it requires only $N + 1$ resolutions of a boundary value problem. The results for both the uniform distribution and the Beta distribution are presented in Figure 4.

We can also use (25) to obtain bounds of intervals of values taken by the Dirichlet energy. In Figure 5, we have plot both the graphs of the functions $J_{\varepsilon,p}^{\pm}$ and the empirical quantiles. Notice that the bounds which are obtained through the asymptotic expansions of the expectation and the variance are better than expected.

Such a nice behavior may depend on the specific choice of Fourier basis, since the shape gradients and Hessian evaluated at the f_N decrease fastly as shown by the following computed values:

$L(f_1) = -0.786069$	$B(f_1, f_1) = -2.35621$
$L(f_2) = -1.74702 \cdot 10^{-6}$	$B(f_2, f_2) = -0.392049$
$L(f_4) = 4.71636 \cdot 10^{-6}$	$B(f_4, f_4) = 0.0246288$
$L(f_6) = 3.00416 \cdot 10^{-7}$	$B(f_6, f_6) = 0.0145671$
$L(f_8) = 4.24149 \cdot 10^{-8}$	$B(f_8, f_8) = 0.00767894$
$L(f_{10}) = -1.48682 \cdot 10^{-7}$	$B(f_{10}, f_{10}) = 0.00440313$

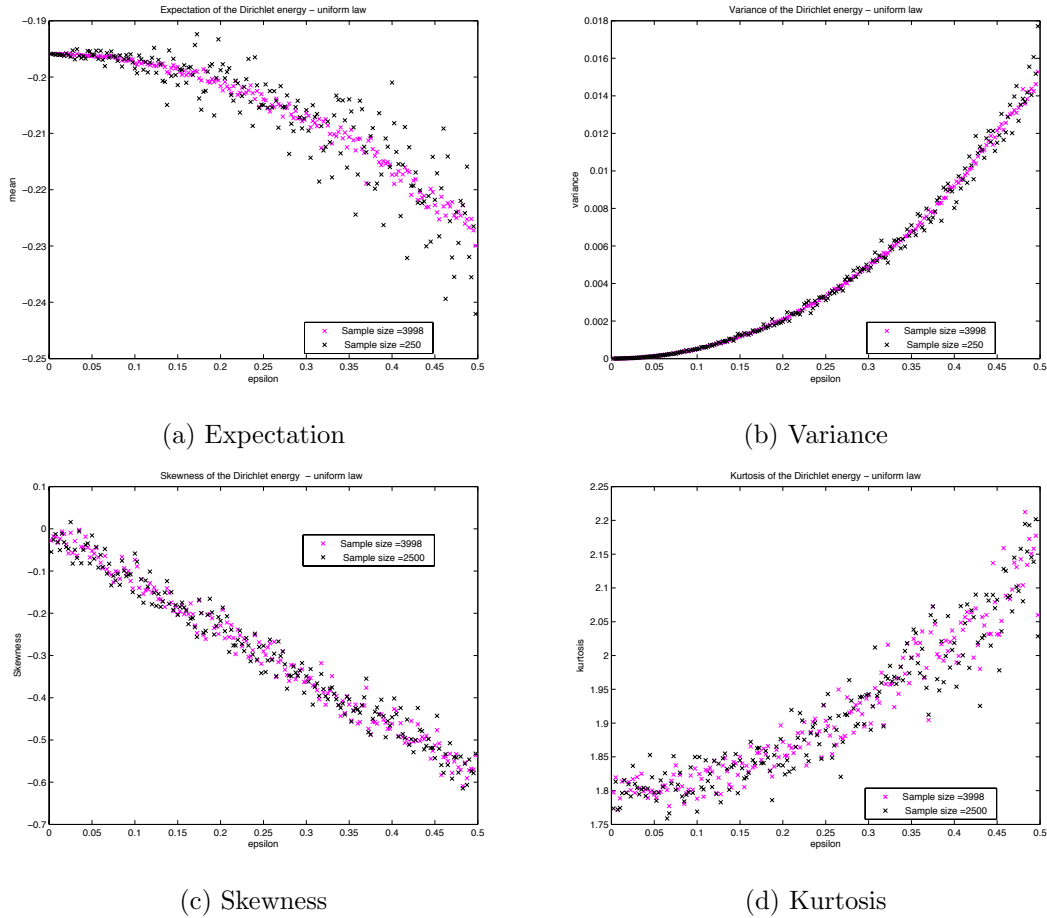


Figure 3: Convergence of Monte-Carlo simulations for perturbed disks defined in (26).

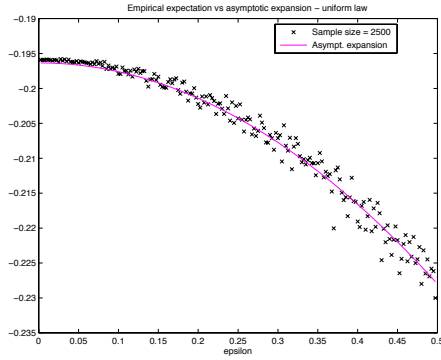
6.1.4 With other boundary perturbations

In this second test, we change the type of random perturbations: instead of being decomposed on Fourier basis, $X(\omega)$ is now described by its zero mean and its covariance function. We shall next consider models with standard covariance kernels, namely Matérn kernels of smoothness class ν . Specifically, we choose $\nu = \infty$ which yields the Gaussian kernel $k_\infty(x, y) = \exp(-|x - y|^2/2)$, we choose $\nu = 1/2$ which yields the exponential kernel $k_{1/2}(x, y) = \exp(-|x - y|)$, and we choose $\nu = 3/2$ which yields the kernel $k_{3/2}(x, y) = (1 - \sqrt{3}|x - y|) \exp(-\sqrt{3}|x - y|)$. The covariance kernels are discretized by 500 periodic cubic B-splines on an equidistant subdivision of $[0, 2\pi]$ in accordance with Subsection 4.3. The pivoted Cholesky decomposition with accuracy 10^{-6} yields a rank of $m = 13$ for k_∞ , a rank of 83 for $k_{3/2}$, and a rank of $m = 500$ for $k_{1/2}$.

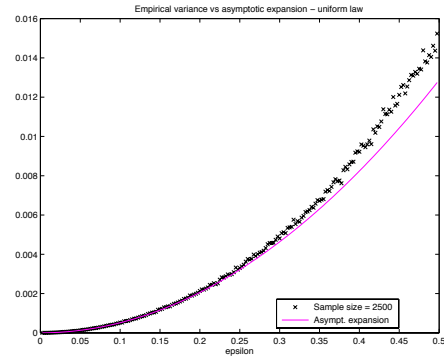
We still compare a Monte-Carlo simulation with the asymptotic expansions derived in this paper for different values $\varepsilon \leq 0.2$. For the Monte-Carlo simulation, we assume that $X(\omega, \theta)$ could be written as the following truncated Karhunen-Loève type expansion:

$$X(\omega, \theta) = \sum_{\aleph=0}^m \alpha_{\aleph}(\omega) \sqrt{\lambda_{\aleph}} \varphi(\theta),$$

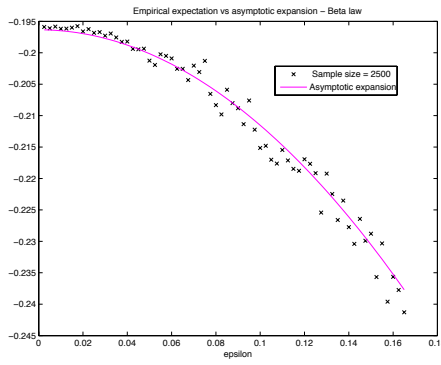
where the random variables are assumed to be i.i.d. and modeled as uniformly distributed in $[-\sqrt{3}, \sqrt{3}]$.



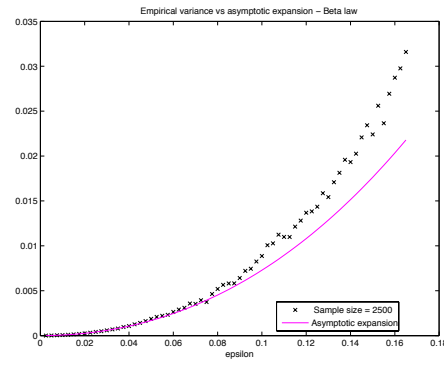
(a) Expectation
Uniform distribution



(b) Variance
Uniform distribution

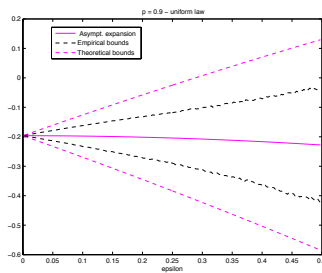


(c) Expectation
Beta distribution

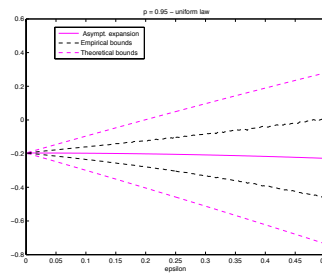


(d) Variance
Beta distribution

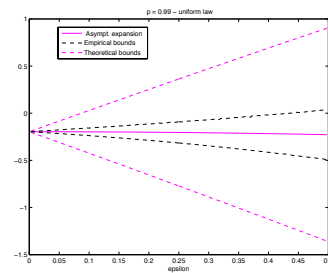
Figure 4: Comparison of the Monte-Carlo simulation with the asymptotic expansions for perturbed disks defined in (26).



(a) $p = 0.9$



(b) $p = 0.95$



(c) $p = 0.99$

Figure 5: Comparison between asymptotic expansions' bounds and empirical quantiles for perturbed disks defined in (26).

Herein, the same accuracy is used as for the pivoted Cholesky decomposition which yields nearly the same ranks m . The numerical computation of the shape functional, shape gradient and shape Hessian is now performed by a fast boundary element method as outlined in [6]. The Monte-Carlo method uses 10 000 samples. As seen in Figures 6, 7, and 8, the asymptotic expansions fit well the behaviour of

the expectation and variance of the stochastic shape functional under consideration for all covariance kernels under consideration.

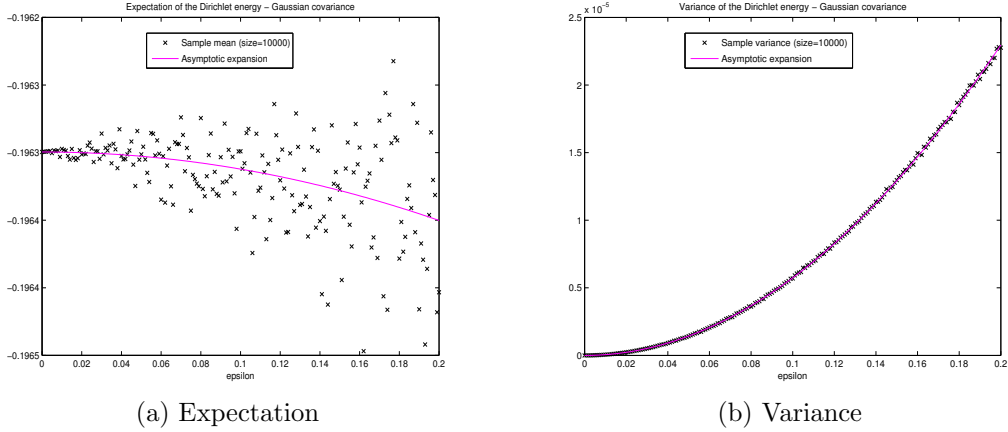


Figure 6: Expectation and variance of the Dirichlet energy – Gaussian covariance kernel k_∞ .

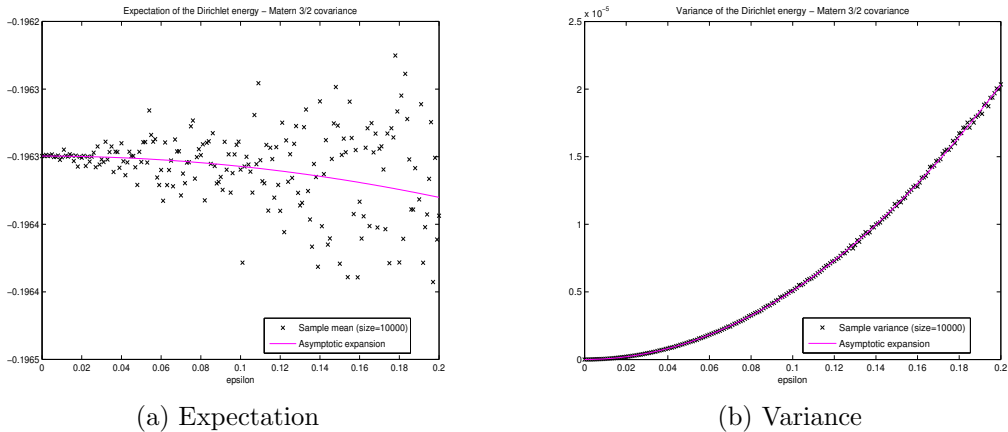


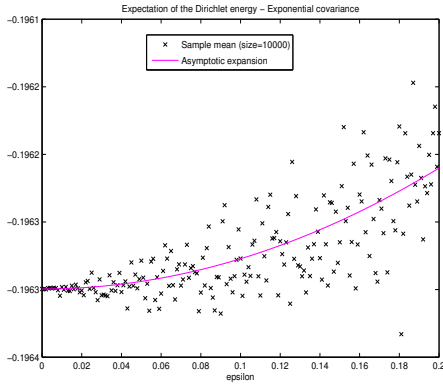
Figure 7: Expectation and variance of the Dirichlet energy – Matern covariance kernel $k_{3/2}$.

6.2 The first eigenvalue of the Laplace Dirichlet operator in a perforated ellipse

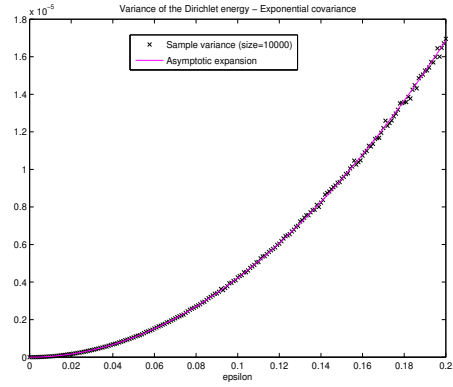
To consider another output function, we present simulations for the first eigenvalue of the Dirichlet Laplace operator. Again, the related shape gradient and Hessian are obtained thanks to Lemma 2.2. Here the reference domain D is an ellipse of semi axis 4 and 3 where a disk centered of the center of the ellipse and of radius 1 are been removed. Random perturbations are applied to the disk's boundary. As in the first example, we take

$$f(\theta) = \sum_{\aleph=1}^N \alpha_{\aleph}(\omega) f_{\aleph}(x)$$

where the α_{\aleph} are i.i.d. In the following computations, we have taken $N = 21$ and the f_{\aleph} are the first normalized functions in the Fourier basis. We emphasize in Figure 9 the local character of the approximation.

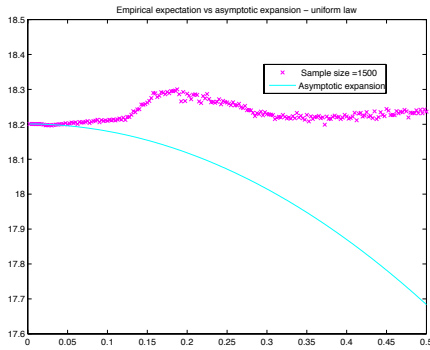


(a) Expectation

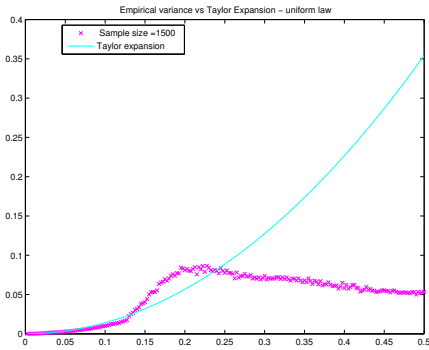


(b) Variance

Figure 8: Expectation and variance of the Dirichlet energy – Exponential covariance kernel $k_{1/2}$.



(a) Expectation



(b) Variance

Figure 9: Comparison between the asymptotic expansions and the Monte-Carlo simulation for the eigenvalue problem – Uniform distribution.

Acknowledgements: The first author thanks support from the ANR through the grants OPTIFORM and ARAMIS. The second author thanks the support of the SNF through the grant “Rapid solution of boundary value problems on stochastic domains”.

References

- [1] A. Chernov and C. Schwab. First order k -th moment finite element analysis of nonlinear operator equations with stochastic data. *Math. Comput.*, 82(284):1859–1888, 2013.
- [2] M. Dambrine. On variations of the shape Hessian and sufficient conditions for the stability of critical shapes. *RACSAM, Rev. R. Acad. Cien. Serie A. Mat.* 96(1):95–121, 2002.
- [3] M. Dambrine and J. Lamboley. Stability in shape optimization with second variation. *Preprint.*, 2014.
- [4] M. C. Delfour and J.-P. Zolésio. *Shapes and geometries*, volume 4 of *Advances in Design and Control*. Society for Industrial and Applied Mathematics (SIAM), Philadelphia, PA, 2001. Analysis, differential calculus, and optimization.
- [5] K. Eppler. Boundary integral representations of second derivatives in shape optimization. *Discuss. Math. Differ. Incl. Control Optim.*, 20:63–78, 2000.

- [6] K. Eppler and H. Harbrecht. Second-order shape optimization using wavelet BEM. *Optim. Methods Softw.*, 21(1):135–153, 2006.
- [7] H. Harbrecht. On output functionals of boundary value problems on stochastic domains. *Math. Methods Appl. Sci.*, 33(1):91–102, 2010.
- [8] A. Henrot and M. Pierre. *Variation et optimisation de formes*, volume 48 of *Mathématiques & Applications (Berlin) [Mathematics & Applications]*. Springer, Berlin, 2005. Une analyse géométrique. [A geometric analysis].
- [9] H. Harbrecht. Second moment analysis for Robin boundary value problems on random domains. In M. Griebel, editor, *Singular Phenomena and Scaling in Mathematical Models*, pages 361–382, Springer, Berlin, 2013.
- [10] H. Harbrecht, M. Peters, and R. Schneider. On the low-rank approximation by the pivoted Cholesky decomposition. *Appl. Numer. Math.*, 62(4):428–440, 2012.
- [11] H. Harbrecht, M. Peters, and M. Siebenmorgen. Combination technique based k -th moment analysis of elliptic problems with random diffusion. *J. Comput. Phys.*, 252:128–141, 2013.
- [12] H. Harbrecht, R. Schneider, and C. Schwab. Sparse second moment analysis for elliptic problems in stochastic domains. *Numer. Math.*, 109(3):385–414, 2008.
- [13] A. Novruzi and M. Pierre. Structure of shape derivatives. *J. Evol. Equ.*, 2(3):365–382, 2002.
- [14] O. Pironneau. *Optimal Shape Design for Elliptic Systems*. Springer, New York, 1983.
- [15] V. Schulz. A Riemannian view on shape optimization. *Found. Comput. Math.*, 14:483–501, 2014.
- [16] C. Schwab and R.A. Todor. Karhunen-Loève approximation of random fields by generalized fast multipole methods. *J. Comput. Phys.*, 217:100–122, 2006.
- [17] J. Sokolowski and J.-P. Zolesio. *Introduction to Shape Optimization*. Springer, Berlin, 1992.
- [18] J. Wloka. *Partial Differential Equations*. Cambridge University Press, Cambridge, 1987.

Marc Dambrine
 Université de Pau et des Pays de l'Adour
 E-mail: marc.dambrine@univ-pau.fr

Helmut Harbrecht
 Universität Basel
 E-mail: helmut.harbrecht@unibas.ch

Bénédicte Puig
 Université de Pau et des Pays de l'Adour
 E-mail: bpuig@univ-pau.fr

LATEST PREPRINTS

No.	Author: Title
2014-01	Helmut Harbrecht, Michael Peters, Markus Siebenmorgen <i>Efficient Approximation of Random Fields for Numerical Applications</i>
2014-02	Ali Hyder, Luca Martinazzi <i>Conformal Metrics on R^{2m} with Constant Q-Curvature, Prescribed Volume and Asymptotic Behavior</i>
2014-03	Jürgen Dölz, Helmut Harbrecht, and Michael Peters <i>H-Matrix Accelerated Second Moment Analysis for Potentials with Rough Correlation</i>
2014-04	Tianling Jin, Ali Maalaoui, Luca Martinazzi, Jingang Xiong <i>Existence and Asymptotics for Solutions of a Non-Local Q-Curvature Equation in Dimension Three</i>
2014-05	Marcus J. Grote, Michaela Mehlin, Teodora Mitkova <i>Runge-Kutta Based Explicit Local Time-Stepping Methods for Wave Propagation</i>
2014-06	Hanspeter Kraft, Andriy Regeta <i>Automorphisms of the Lie Algebra of Vector Fields on Affine n-Space</i>
2014-07	Jérémy Blanc, Alberto Calabri <i>On Degenerations of Plane Cremona Transformations</i>
2014-08	Helmut Harbrecht, Michael Peters, Markus Siebenmorgen <i>Numerical Solution of Elliptic Diffusion Problems on Random Domains</i>
2014-09	H. Harbrecht, W.L. Wendland, and N. Zorii <i>Rapid Solution of Minimal Riesz Energy Problems</i>
2014-10	Julien Diaz, Marcus J. Grote <i>Multi-Level Explicit Local Time-Stepping Methods for Second-Order Wave Equations</i>
2014-11	J. Dölz, H. Harbrecht, Ch. Schwab <i>Covariance Regularity and H-Matrix Approximation for Rough Random Fields</i>
2014-12	Giovanni Alberti, Gianluca Crippa, Anna L. Mazzucato <i>Exponential Self-Similar Mixing and Loss of Regularity for Continuity Equations</i>

LATEST PREPRINTS

No. **Author:** *Title*

2014-12 **Giovanni Alberti, Gianluca Crippa, Anna L. Mazzucato**
Exponential Self-Similar Mixing and Loss of Regularity for Continuity Equations